Review

Combining Neural Networks and Genetic Algorithms to Understand Composition–Microstructure–Property Relationships in Additively Manufactured Metals

Sooraj Patel, Anvesh Nathani, Amin Poozesh, Shuozhi Xu [ID], Pejman Kazempoor and Iman Ghamarian *

School of Aerospace and Mechanical Engineering, University of Oklahoma, Norman, OK 73019, USA; sooraj.patel@ou.edu (S.P.)
* Correspondence: iman@ou.edu

Abstract: Additive manufacturing (AM) has revolutionized the production of complex metallic components by enabling the direct fabrication of intricate geometries from 3D model data. Despite its advantages in reducing material waste and customization of mechanical properties, AM faces challenges related to microstructural heterogeneity and mechanical property variability. This review highlights the structure–property relationships in additively manufactured metals, emphasizing how heterogeneous microstructure influences yield strength and fracture toughness. Phenomenological equations are provided based on the integration of neural networks and genetic algorithm-based models to predict mechanical properties from composition and microstructural features. We also outline key considerations such as acquiring high-fidelity datasets and understanding mathematical correlations within the data needed to formulate phenomenological equations.

Keywords: neural networks; genetic algorithms; phenomenological equation; titanium alloys

1. Introduction

Additive manufacturing (AM) encompasses a diverse array of techniques engineered to fabricate complex metallic components with exceptional precision [1]. By employing controlled melting and solidification during layer-by-layer deposition, AM enables the construction of intricate geometries directly from computed models, significantly accelerating the transition from design to finished parts [2]. AM minimizes material waste by employing a layer-by-layer deposition process, which ensures precise material utilization. Unlike conventional subtractive methods, AM enables near-net-shape fabrication, reducing excess material removal [3]. Moreover, the flexibility of AM extends to the spatial variation of composition and microstructure within a component, allowing for the local customization of mechanical properties to meet specific performance requirements. These advantages make AM a transformative technology in various fields, including biomedical applications [4,5], aerospace and automobile components [6], and oil and gas industries [7].

The structural properties of AM products are primarily determined by processing parameters and the microstructural features developed during solidification. Rapid solidification rates (up to 10^4 K/s [8] or 10^5 K/s [9]) render AM processes far from equilibrium. Additionally, cyclic melting [10] and non-uniform thermal histories over successive layer depositions [11] complicate microstructural predictions. These challenges give rise to several issues in AM products, including residual stresses, structural distortion, pore formation [12], and phase transformations [13]. Variations in heat flux during the deposition process lead to significant changes in the grain growth direction of printed parts [14]. Notably, the literature reports considerably different microstructures, primarily because microstructure formation depends on the location within the sample [15], where different thermal histories occur. Local heterogeneity in composition and microstructure complicates structure–property investigations in additively manufactured parts.

Although a significant body of work exists on studying microstructural evolutions in additively manufactured metals [16,17], exploring the phenomenological models is limited in elucidating the relationships between composition, microstructure, and mechanical properties of 3D-printed components [18]. One of the key challenges is collecting the required high-fidelity information that covers all key parameters and represents the majority of governing mechanisms. AM parameters influence several attributes, including fluid dynamics, thermal distribution, chemical reactions, solidification and phase transformation, deformation, and shrinkage. However, optimizing these parameters is challenging due to their nonlinear interactions. Adjusting one parameter can lead to complex changes in others, resulting in intricate variations in material properties. The complex relationships between variables and their impact on the output make data collection challenging. For instance, it is nearly impossible to change one microstructural variable while keeping others constant. In other words, it is challenging to experimentally isolate the effect of a single variable on the output without interference from other variables [19].

This paper highlights the structure–property relationships in additively manufactured metals, focusing on how microstructural evolutions during the manufacturing process influence key mechanical properties. It further reviews phenomenological models for predicting yield strength based on microstructural characteristics and compositional factors using the integration of neural networks (NNs) with genetic algorithms (GAs). Such a model helps predict the independent role of each parameter affecting the resultant property. This study provides a framework for developing NN- and GA-based models to predict the mechanical properties from composition and microstructural features. It outlines key considerations in developing such models, including (i) acquiring high-fidelity datasets, (ii) discerning the mathematical correlations within the data, and (iii) formulating phenomenological equations.

2. Structure–Property Relationship

While the ability to fabricate intricate geometries directly from virtual designs makes AM fascinating, the mechanical properties of AM-fabricated components are of paramount importance, especially considering their applications in the aerospace industry. A wide variation in mechanical properties such as yield strength, toughness, and fatigue resistance has been reported in AM products. These variations are subject to the selected AM methods, composition, process parameters, build orientation, and post-heat treatments [20–22]. For instance, the tensile strength of AM-fabricated samples is orientation-dependent and significantly varies with respect to the build direction [23]. Such variations in mechanical properties make AM-fabricated components less reliable for sensitive applications like aerospace components. This variability has driven research efforts toward understanding the underlying microstructural features that contribute to these mechanical property differences.

The rapid and localized directional solidification during each layer deposition leads to the development of grains with preferred orientation, scientifically known as texture [24]. This texture persists across multiple layers, forming high-aspect-ratio grains that follow the solidification direction. Columnar grains formed across multiple deposited layers are schematically presented in Figure 1a. The preference for solidification growth in a particular direction is attributed to differences in free energy at the solid–liquid interface and the stiffness of different crystallographic planes at the interface. Furthermore, as the direction of beam energy deflects the thermal gradient, the columnar growth deviates angularly based on the scanning direction, leading to columnar growth with multiple deviations attributed to the scanning direction of each layer [25]. Since dislocation climb and cross-slips are crystallographic orientation-dependent, the mechanical properties are highly influenced by texture. This leads to anisotropy in mechanical properties with respect to the direction of deposition. Figure 1b demonstrates the variation in hardness within the deposited layers in an additively printed α/β titanium part. Such heterogeneity in hardness further necessitates detailed microstructural characterization to understand the mechanical response and performance of additively manufactured metallic materials.
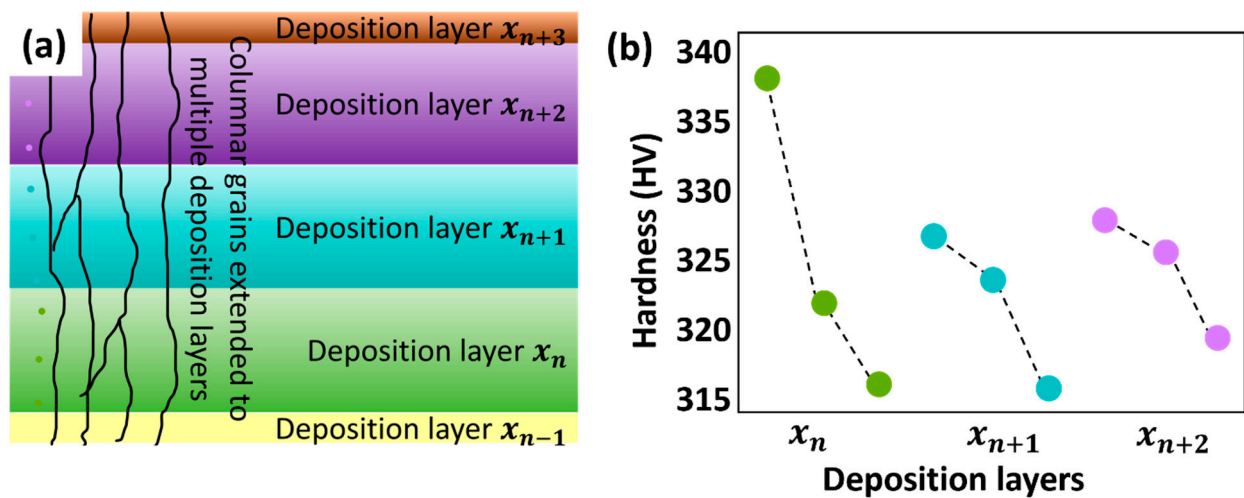
Figure 1. Considerable variations in microstructure can be a reason for location-dependent properties. (**a**) A schematic representing columnar grains formed across multiple deposited layers; (**b**) hardness variation within the deposited layers in an additively printed α/β titanium part.

Rapid solidification and post-heat treatments in the AM of multicomponent systems provide a wide scope for the formation of thermodynamically stable or metastable phases, including martensitic phases, bulk metallic glasses, and eutectic structures. For example, in laser-deposited Ti-6Al-4V, elongated prior β grains [26], as well as the coexistence of equiaxed α and basketweave microstructures, have been observed [15]. In the case of electron beam deposition, a very fine α/β lamellar microstructure was observed [27,28]. It has been shown that Widmanstätten morphology grows in columnar prior β grains [9,29], containing a martensitic α' phase [9]. In directed energy deposition, a fine Widmanstätten microstructure was reported in a Ti-6Al-4V deposited sample [30]. Furthermore, post-heat treatments or certain AM methods allow for the precipitation of uniformly distributed precipitates, significantly affecting precipitation hardening [31–34]. The presence of multiple phases and precipitation hardening significantly affects deformation characteristics and, consequently, mechanical properties such as yield strength and toughness.

There is considerable uncertainty in the mechanical properties of additively manufactured metallic materials. These uncertainties are attributed to heterogeneity in microstructure and composition or the formation of defects during deposition. To increase the reliability of additively manufactured materials, we should (1) quantitatively assess the contributions of microstructure, composition, and defects to mechanical properties, and (2) tune the processing parameters to achieve the desired microstructure and composition that lead to the desired mechanical properties and performance. However, the nonlinear relationships among processing parameters impose significant challenges in experimental optimization. To address this issue, well-trained phenomenological models integrated with neural networks (NNs) and genetic algorithms (GAs) have been applied to enhance the desired properties by tuning these parameters.

3. Model Development

The integration of NN with GA optimizes the desired property by training a multiparameter model, applying genetic operations, and running the algorithm until the desired property reaches an optimal or near-optimal NN configuration. Notably, NNs have been used in many applications, such as predicting the mechanical response and phase transformations of titanium alloys [35–41], nickel [42], and steel [43–48]. GAs have also been applied to many materials science problems to find the best parameters involved in a mechanism [49,50] and to model the evolution of microstructure [51,52]. GAs have been combined with NNs to tune predictions [53–55]. For example, the heat treatment procedure

for the AA7175 aluminum alloy can be modified based on the expected properties and performance by combining NNs with GAs [56].

3.1. Collecting High-Fidelity Datasets

NNs require high-fidelity datasets to effectively model complex systems, especially when predicting mechanical properties influenced by microstructure and chemical composition. The accuracy of these models hinges on the adjustment of internal weights during training, which requires robust and diverse datasets to capture the full spectrum of material variations, minimize bias, and prevent overfitting. In investigating structure–property relationships, datasets must cover a broad range of input parameters, including variations in chemical composition (e.g., concentrations of alloying elements) and microstructural features (e.g., phase fractions, precipitate size, distribution, crystal orientation, and grain morphology). Microstructural characteristics, such as columnar, equiaxed, dendritic, or twinned grains, directly influence mechanical properties such as yield strength, toughness, and fatigue resistance. Therefore, to ensure comprehensive coverage of material behavior, multiple dataset entries must represent each combination of composition and microstructure.

Experimentally exploring the entire range of input parameters to develop such datasets poses significant challenges. Despite this, researchers have successfully generated high-fidelity datasets by selectively varying key input parameters and measuring corresponding mechanical properties. For instance, Collins et al. [41,57] developed a dataset for α-β titanium alloys by adjusting the concentrations of aluminum, vanadium, iron, and oxygen, and applying thermomechanical treatments above and below the phase transformation temperature. They measured tensile strength for each condition, providing valuable insights into the relationship between composition, microstructure, and mechanical properties, emphasizing α-phase size and morphology. Similarly, Kusano et al. [58] generated a dataset by varying solution treatment times and temperatures to correlate microstructural features (grain size, aspect ratios, and pore characteristics) with tensile properties. These studies demonstrate how targeted experimental designs can yield valuable datasets, even when a full parameter space exploration is impractical.

Characterization techniques, particularly X-ray methods such as synchrotron X-ray tomography, X-ray diffraction, and scattering, are useful in generating high-fidelity datasets for machine learning models to obtain insights into microstructural features and chemical compositions [59–61]. Rezasefat et al. [62] performed X-ray micro-computed tomography scans of alumina and analyzed them to identify porosities, impurities, and the 3D microstructural geometry of the material. These data were processed to threshold segmentation, reconstruct the 3D inclusions, and analyze their volume, aspect ratio, and distribution. The 3D morphological data derived from the CT scans were used to create FE models, where simulations were performed to predict stress–strain responses and progressive damage.

Datasets for NN training can be expanded using physics-based simulations [63] and finite element methods [64], which predict microstructure-dependent mechanical properties. Dai et al. [65] generated the data using the visco-plastic self-consistent model. This model simulated datasets of stress, strain, and grain orientations (texture) for copper under different load conditions (e.g., uniaxial tension, compression, and simple shear). By integrating both experimental and simulation-generated data, researchers can develop more comprehensive and versatile datasets, ultimately improving the predictive accuracy of machine learning models.

3.2. Establishing the Mathematical Relationships Between the Collected Data

To elucidate mathematical relationships within the collected datasets, the model utilizes the majority of the data for training while reserving a smaller portion for testing the NN analysis. In our work, a model based on MacKay's Bayesian NN code [66,67] serves as a primary basis for training NNs. Figure 2 shows a schematic of an NN model with input and output parameters. The intermediate layers are the hidden layers represented by the circles between the input and output layers. They consist of neurons that apply

transformations to input data using learned weights and biases, followed by an activation function. These layers enable the network to capture complex patterns and relationships within the data. In the model presented by Dai et al. [65], the architecture has multiple layers with hyperbolic tangent activation functions between layers.
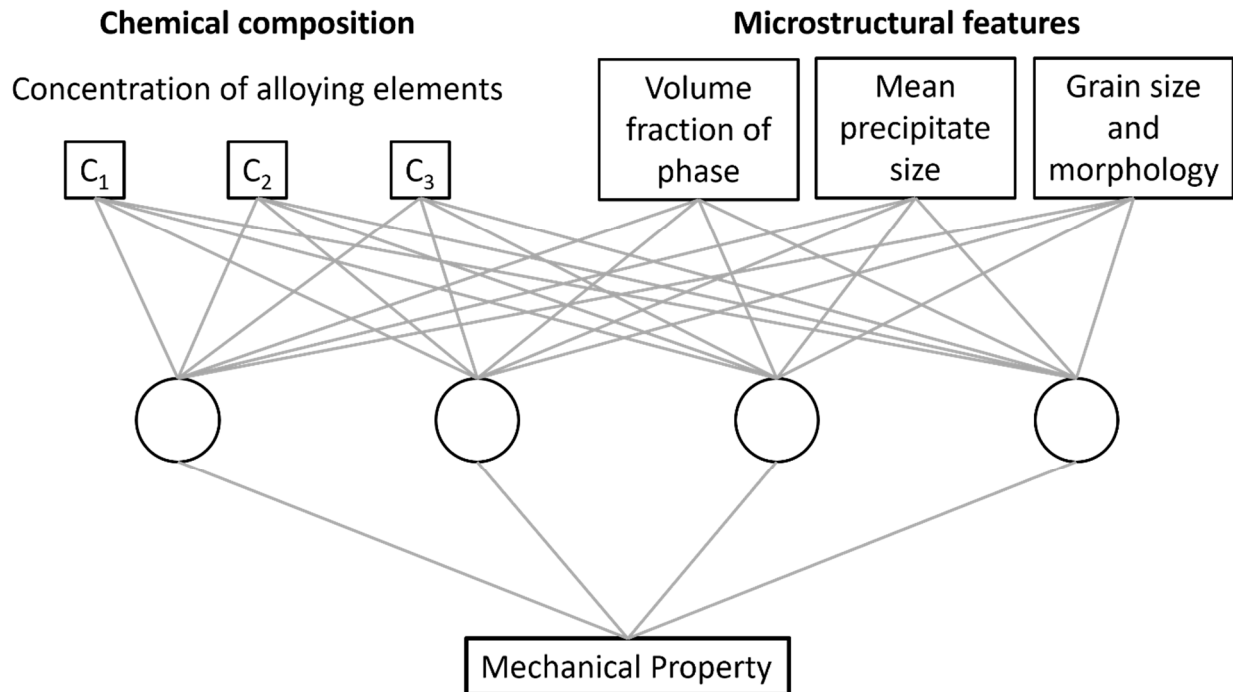
Figure 2. Schematic representation of neural network model of composition–structure–property relationships. C_1, C_2, and C_3 refer to the concentration of alloying elements in a multicomponent material.

To mathematically study the impact of each compositional and microstructural variable on the mechanical properties, the trained NN model was applied to synthetic datasets. These datasets were generated by varying only one variable over its experimental range while keeping the other variables fixed at constant values (e.g., mean values). From the experimental data alone, it is impossible to draw clear conclusions about the effect of one input parameter on the output (e.g., the effect of equiaxed alpha size on yield strength) because changing one variable leads to variations in other variables that affect the microstructure. However, the results of virtual experiments using NN provide the opportunity to show the impact of each variable on the output while the other variables are held constant.

While NN models are very flexible and can capture complex relationships between inputs and outputs, these models are not readily interpretable. The lack of interpretability arises because NNs are composed of mathematical functions (e.g., summation and hyperbolic tangent functions) without explicit physical meaning.

3.3. Establishing the Phenomenological Equation

Figure 3 presents the method for establishing the phenomenological equation from a dataset. The NNs capture the complex relationships between the inputs and outputs, followed by virtual experiments using the well-trained NN model. Virtual experiment databases are generated by changing each variable from its minimum to its maximum measured value while keeping other variables at their average values.
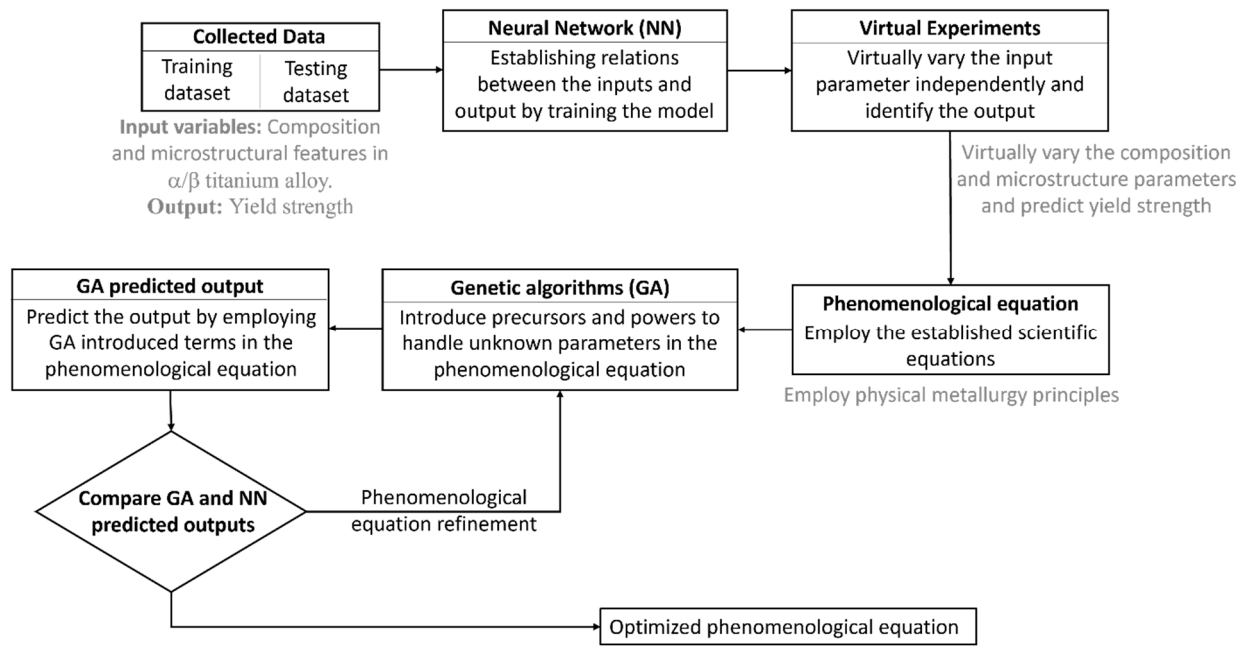
Figure 3. Procedure to develop phenomenological equations from an experimental dataset.

While NN models can accurately predict properties, their complexity makes physical interpretation difficult. GA addresses this by deriving more interpretable phenomenological equations based on physical metallurgy principles. For instance, it can be assumed that in single-phase metallic alloys, the contribution of composition to strengthening can be attributed to the intrinsic strength of the material, solid solution strengthening, and grain boundary strengthening (Hall–Petch relation). In multi-phase metallic systems, the phenomenological equation includes additional terms such as particle strengthening and precipitation hardening. Voigt and Reuss models are introduced in multi-phase systems to predict the elastic properties [68]. The model to define crystal plasticity considers material properties such as strain hardening and dynamic recovery [69].

The unknown parameters in the phenomenological equation are the coefficients and exponents. These unknown parameters are determined using the GA method. GA is an optimization method that can find the optimum values for the unknown coefficients and exponents to minimize the difference between the NN and GA predictions. The phenomenological equation is modified iteratively by adding new terms to reduce the difference between the NN and GA predictions and removing terms that have a small contribution to the estimated yield strength values. The models were designed to capture both continuum variables (such as yield strength and reduction in area) and micromechanistic details (like microcracking and void nucleation). The models underwent virtual experiments to explore how each variable functionally depended on the predicted toughness, which helped establish the phenomenological relationships [57].

Even though multiple iterations are performed on the phenomenological equation during the refinement of coefficients and exponents, it is important to consider that a lack of accuracy in NN and GA predictions can be observed for certain parameters. Such inaccuracies can be attributed to factors that might not be considered in the model. The limitations of virtual experiments must be acknowledged, as simulation models are inherently unable to fully capture real-world complexities. To enhance predictive accuracy, additional equations need to be considered to quantitatively map critical parameters, such as the distribution of densities of geometrically necessary dislocations and texture. Hayes et al. [70] addressed this challenge by optimizing phenomenological equations for yield strength prediction, incorporating these parameters (Table 1). The refinement of coefficients and exponents over multiple iterations is included in the relevant strengthening equations. Here, the relationship between dislocation density and the resulting material hardening is

described by the Taylor hardening term. Xie et al. [71] introduced a data-driven approach that integrates the concept of dimensional invariance within a hierarchical machine learning model to identify the dominant dimensionless parameters underlying governing principles from the limited experimental results.

Table 1. The optimized phenomenological equation [70]. F_V, C, and t represent the volume fraction, concentration, and thickness, respectively. In the Taylor hardening term, G, b, and r are shear modulus, Burgers vector, and dislocation density, respectively.

Yield Strength $\sigma_y=$	$\left(89 \times F_V^\alpha\right) + \left(45 \times F_V^\beta\right) +$	Intrinsic strength
	$F_V^\alpha \times \left(149 \times C_{Al}^{0.667} + 759 \times C_O^{0.667}\right)+$	Solid solution strengthening (alpha phase)
	$F_V^\beta \times \left(\left(22 \times C_V^{0.7}\right)^{0.5} + \left(235 \times C_{Fe}^{0.7}\right)^{0.5}\right)^2 +$	Solid solution strengthening (beta phase)
	$F_V^{col} \times 150 \times \sqrt{\dfrac{t_{\beta-rib}}{t_{\alpha-lath}}} +$	Hall–Petch strengthening (alpha laths)
	$F_V^{col} \times 125 \times t_{colony}^{-0.5} +$	Hall–Petch strengthening (colonies)
	$F_V^{BW} \times \alpha MGb\sqrt{\rho} -$	Taylor hardening
	AxisDebit	Texture debits (easier slip)

NN and GA synergistically enable autonomous experimental loops by combining predictive modeling and optimization capabilities. NN predicts material properties or synthesis outcomes based on experimental conditions, significantly reducing the need for exhaustive trial-and-error experiments. These models can be iteratively improved by integrating active learning strategies, wherein new experimental data are selectively acquired from regions of high uncertainty or interest, as identified by the NN. GA complements this framework by optimizing experimental parameters to meet target objectives, such as maximizing a desired property or minimizing resource use. In this context, the GA acts as an optimizer, leveraging the predictions of the NN to guide the selection and evolution of candidate experiments. This loop is further enhanced by using Bayesian optimization within the GA to balance exploration and exploitation. The autonomous system continuously refines itself by feeding experimental outcomes into the NN for retraining, creating a closed-loop system that accelerates material discovery and design. This approach offers substantial efficiency gains by prioritizing the most informative experiments and leveraging machine learning for dynamic adaptation during the discovery process [72].

3.4. Model Performance

The performance of the NN and GA models is evaluated by comparing predicted outputs against experimental values. Testing is performed with separate datasets (e.g., 15–20% of the total data) to ensure the ability of the model to generalize beyond the training set. The performance of the NN model is evaluated based on its agreement with the experimental values of testing datasets. The key metrics used for evaluation include the mean square error (MSE), average deviation, and maximum deviation between predicted and experimental values. Correlation coefficients are utilized to measure the fitting of predicted values with actual values. Multiple NN architectures are tested to improve performance evaluation, and the models with the lowest MSEs are selected for further interrogation.

The GA is combined with NNs to refine a complex mathematical function derived from the NN model, allowing it to minimize the difference between the model predictions and experimental data. The GA iteratively modifies the predictions and selects the fittest ones based on predefined rules. Over successive iterations, GA evolves toward an optimal solution that minimizes the error between the predicted and measured mechanical properties. The accuracy of the model was validated by conducting virtual experiments exploring the influence of input variables (composition, microstructure, etc.) on mechanical properties (tensile strength, fracture toughness, etc.).

3.4.1. Performance in α + β Titanium Alloys

Predicting the mechanical properties of the α + β titanium alloy Ti-6Al-4V remains a complex challenge due to its intricate two-phase microstructure, characterized by the coexistence of hexagonal close-packed α-phase and body-centered cubic β-phase. The integration of NN, GA, and Monte Carlo (MC) simulations has proven effective in developing robust phenomenological models for these alloys. These models accurately incorporate various strengthening mechanisms, including intrinsic phase strength, solid solution strengthening, Hall–Petch effects, and the influence of basketweave microstructures.

Figure 4 illustrates the virtual compositional and microstructural dependencies affecting the yield strength of Ti-6Al-4V, as predicted using NN and GA models. Oxygen exhibited the strongest contribution to strengthening, followed by iron, aluminum, and vanadium, which is consistent with established trends in solid solution strengthening. Regarding microstructural factors, the grain size of the equiaxed α-phase and the volume fraction of the total α-phase were identified as key determinants of yield strength. Finer grain sizes and greater α-phase volume fractions enhance yield strength through Hall–Petch strengthening mechanisms. The strong correlation between neural network predictions and the phenomenological model underscores the accuracy of these models in predicting yield strength based on critical microstructural and compositional variables [73].
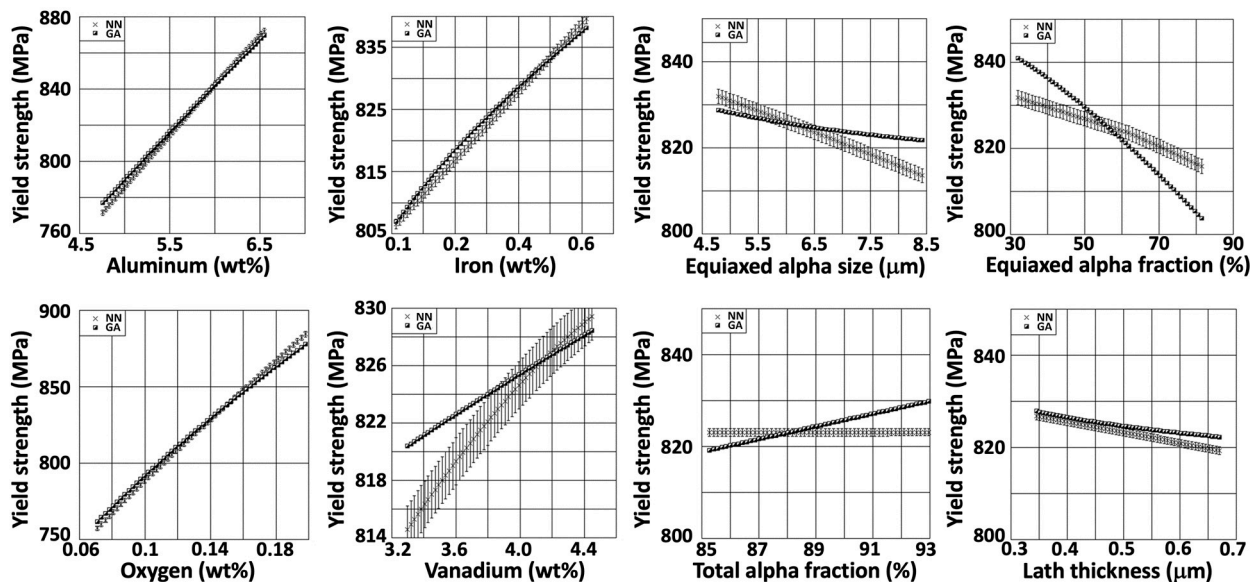
Figure 4. Virtual experiment results for the NN and GA analyses of the composition and microstructure variables in α + β titanium alloy Ti-6Al-4V [73]. Reproduced with permission from Springer Nature (2015).

The relationship between yield strength and fracture toughness in Ti-6Al-4V typically follows an inverse pattern, where increases in yield strength generally compromise the material's resistance to crack propagation. Fracture toughness predictions were refined by incorporating key microstructural features, such as the size of equiaxed α-phase grains and the volume fraction of the α-phase, alongside variations in chemical composition. The α-stabilizing elements, such as aluminum, significantly influence fracture toughness through their role in enhancing yield strength. In contrast, β-stabilizing elements, including vanadium and iron, exhibit more complex and nuanced effects on mechanical behavior. Interestingly, iron has been observed to contribute positively to both yield strength and fracture toughness, which is atypical compared to other alloying elements. The average deviation between predicted and experimental fracture toughness values has been significantly minimized, with reductions to as low as 0.9% and a maximum deviation of 5.8% [57].

3.4.2. Performance in β Titanium Alloys

The optimized NN-GA model predicted yield strength with a maximum error of 5%, providing an interpretable phenomenological equation that aligns with physical metallurgy principles, incorporating intrinsic yield strength, solid solution strengthening, Hall–Petch effects, and microstructural contributions. MC simulations showed that uncertainties in variables such as aluminum content caused minor deviations in the yield strength estimates. However, the NN-GA model consistently provided accurate predictions. Although microstructural features like α-lath thickness and colony size influence strengthening, the model identified solid solution strengthening, particularly from aluminum and oxygen, as the primary contributor to yield strength, accounting for approximately 78% in β titanium alloys. The phenomenological equation for β-processed alloys was similar to that of α + β-processed alloys, but key differences were observed due to the absence of equiaxed α microstructures in β-processed alloys and the stronger influence of the basketweave microstructure [74].

4. Summary

AM presents substantial opportunities for the production of complex metallic components with tailored properties. However, the variability in mechanical properties, resulting from microstructural heterogeneity, introduces challenges for the reliable application of AM in critical industries such as aerospace. This review emphasizes the significance of understanding the structure–property relationships in additively manufactured metals and examines the influence of microstructural evolution in single- and multi-phase titanium alloys on their mechanical properties. It highlights the critical need for the development of comprehensive models to predict these structure–property relationships accurately.

Integrating NN with GA effectively models the complex, nonlinear relationships between processing parameters, microstructure, and mechanical properties. By leveraging high-fidelity datasets and analyzing the mathematical correlations within the data, phenomenological equations can be formulated to predict material behavior accurately. The combination of NNs and GAs facilitates the optimization of these models, improving predictive accuracy and enabling the tuning of processing parameters to achieve desired properties. This progress is critical for the broader adoption of AM technologies in industries where material performance is of paramount importance.

Author Contributions: Conceptualization, S.P. and I.G.; writing-original draft, S.P.; writing-review and editing, A.N., A.P., S.X., P.K. and I.G.; visualization, I.G.; supervision, I.G.; funding acquisition, I.G. All authors have read and agreed to the published version of the manuscript.

Data Availability Statement: No new data were created.

Conflicts of Interest: The authors declare no conflict of interest.

References

1. Wong, K.V.; Hernandez, A. A review of additive manufacturing. *Int. Sch. Res. Not.* **2012**, *2012*, 208760. [CrossRef]
2. *ASTM F2792-10e1*; Standard Terminology for Additive Manufacturing Technologies. ASTM International: West Conshohocken, PA, USA, 2012.
3. Patel, S.; Liu, Y.; Siddique, Z.; Ghamarian, I. Metal additive manufacturing: Principles and applications. *J. Manuf. Process.* **2024**, *131*, 1179–1201. [CrossRef]
4. Murr, L. Additive manufacturing of biomedical devices: An overview. *Mater. Technol.* **2018**, *33*, 57–70. [CrossRef]
5. Jardini, A.L.; Larosa, M.A.; Maciel Filho, R.; de Carvalho Zavaglia, C.A.; Bernardes, L.F.; Lambert, C.S.; Calderoni, D.R.; Kharmandayan, P. Cranial reconstruction: 3D biomodel and custom-built implant created using additive manufacturing. *J. Cranio-Maxillofac. Surg.* **2014**, *42*, 1877–1884. [CrossRef]

6. Gradl, P.; Tinker, D.C.; Park, A.; Mireles, O.R.; Garcia, M.; Wilkerson, R.; Mckinney, C. Robust metal additive manufacturing process selection and development for aerospace components. *J. Mater. Eng. Perform.* **2022**, *31*, 6013–6044. [CrossRef]

7. Zhong, A.; Ornelaz, R.; Krishnan, K. Exploration of Applications of Metallic Additive Manufacturing for the Oil and Gas Industry. In Proceedings of the Offshore Technology Conference, Houston, TX, USA, 1–4 May 2017.

8. Zheng, B.; Zhou, Y.; Smugeresky, J.; Schoenung, J.; Lavernia, E. Thermal behavior and microstructural evolution during laser deposition with laser-engineered net shaping: Part I. Numerical calculations. *Metall. Mater. Trans. A* **2008**, *39*, 2228–2236. [CrossRef]

9. Al-Bermani, S.; Blackmore, M.; Zhang, W.; Todd, I. The Origin of Microstructural Diversity, Texture, and Mechanical Properties in Electron Beam Melted Ti-6Al-4V. *Metall. Mater. Trans. A* **2010**, *41*, 3422–3434. [CrossRef]

10. Kelly, S.; Kampe, S. Microstructural evolution in laser-deposited multilayer Ti-6Al-4V builds: Part II. Thermal modeling. *Metall. Mater. Trans. A* **2004**, *35*, 1869–1879. [CrossRef]

11. Singh, A.K.; Mundada, Y.; Bajaj, P.; Wilms, M.B.; Patil, J.P.; Mishra, S.K.; Jägle, E.A.; Arora, A. Investigation of temperature distribution and solidification morphology in multilayered directed energy deposition of Al-0.5 Sc-0.5 Si alloy. *Int. J. Heat Mass Transf.* **2022**, *186*, 122492. [CrossRef]

12. Brennan, M.; Keist, J.; Palmer, T. *Defects in Metal Additive Manufacturing Processes*; Springer: Berlin/Heidelberg, Germany, 2021.

13. Frazier, W.E. Metal Additive Manufacturing: A Review. *J. Mater. Eng. Perform.* **2014**, *23*, 1917–1928. [CrossRef]

14. Thijs, L.; Verhaeghe, F.; Craeghs, T.; Humbeeck, J.V.; Kruth, J.-P. A study of the microstructural evolution during selective laser melting of Ti–6Al–4V. *Acta Mater.* **2010**, *58*, 3303–3312. [CrossRef]

15. Kelly, S.; Babu, S.; David, S.; Zacharia, T.; Kampe, S. A thermal and microstructure model for laser deposition of Ti-6Al-4V. In *Cost-Affordable Titanium, Dedicated to Professor Harvey Flower*; Charoltte: Minerals, Metals and Materials Society; TMS: Hoboken, NJ, USA, 2004; pp. 45–52.

16. Thijs, L.; Montero Sistiaga, M.L.; Wauthle, R.; Xie, Q.; Kruth, J.-P.; Van Humbeeck, J. Strong morphological and crystallographic texture and resulting yield strength anisotropy in selective laser melted tantalum. *Acta Mater.* **2013**, *61*, 4657–4668. [CrossRef]

17. Murr, L.E.; Martinez, E.; Pan, X.M.; Gaytan, S.M.; Castro, J.A.; Terrazas, C.A.; Medina, F.; Wicker, R.B.; Abbott, D.H. Microstructures of Rene 142 nickel-based superalloy fabricated by electron beam melting. *Acta Mater.* **2013**, *61*, 4289–4296. [CrossRef]

18. Quintana, M.J.; Temple, A.J.; Harlow, D.G.; Collins, P.C. On the Prediction of Uniaxial Tensile Behavior Beyond the Yield Point of Wrought and Additively Manufactured Ti-6Al-4V. *Integr. Mater. Manuf. Innov.* **2022**, *11*, 327–338. [CrossRef]

19. Moges, T.; Ameta, G.; Witherell, P. A review of model inaccuracy and parameter uncertainty in laser powder bed fusion models and simulations. *J. Manuf. Sci. Eng.* **2019**, *141*, 040801. [CrossRef] [PubMed]

20. Kok, Y.; Tan, X.P.; Wang, P.; Nai, M.; Loh, N.H.; Liu, E.; Tor, S.B. Anisotropy and heterogeneity of microstructure and mechanical properties in metal additive manufacturing: A critical review. *Mater. Des.* **2018**, *139*, 565–586. [CrossRef]

21. Farabi, E.; Klein, T.; Schnall, M.; Primig, S. Effects of high deposition rate during cold metal transfer additive manufacturing on microstructure and properties of Ti-6Al-4V. *Addit. Manuf.* **2023**, *71*, 103592. [CrossRef]

22. Lu, J.; Zhuo, L. Additive manufacturing of titanium alloys via selective laser melting: Fabrication, microstructure, post-processing, performance and prospect. *Int. J. Refract. Met. Hard Mater.* **2023**, *111*, 106110. [CrossRef]

23. Dixit, S.; Liu, S.; Murdoch, H.A.; Smith, P.M. Investigating build orientation-induced mechanical anisotropy in additive manufacturing 316L stainless steel. *Mater. Sci. Eng. A* **2023**, *880*, 145308. [CrossRef]

24. Hagihara, K.; Nakano, T. Control of anisotropic crystallographic texture in powder bed fusion additive manufacturing of metals and ceramics—A review. *Jom* **2022**, *74*, 1760–1773. [CrossRef]

25. Collins, P.; Brice, D.; Samimi, P.; Ghamarian, I.; Fraser, H. Microstructural control of additively manufactured metallic materials. *Annu. Rev. Mater. Res.* **2016**, *46*, 63–91. [CrossRef]

26. Kelly, S.; Kampe, S. Microstructural evolution in laser-deposited multilayer Ti-6Al-4V builds: Part I. Microstructural characterization. *Metall. Mater. Trans. A* **2004**, *35*, 1861–1867. [CrossRef]

27. Facchini, L.; Magalini, E.; Robotti, P.; Molinari, A. Microstructure and mechanical properties of Ti-6Al-4V produced by electron beam melting of pre-alloyed powders. *Rapid Prototyp. J.* **2009**, *15*, 171–178. [CrossRef]

28. Safdar, A.; Wei, L.-Y.; Snis, A.; Lai, Z. Evaluation of microstructural development in electron beam melted Ti-6Al-4V. *Mater. Charact.* **2012**, *65*, 8–15. [CrossRef]

29. Murr, L.E.; Esquivel, E.V.; Quinones, S.A.; Gaytan, S.M.; Lopez, M.I.; Martinez, E.Y.; Medina, F.; Hernandez, D.H.; Martinez, E.; Martinez, J.L.; et al. Microstructures and mechanical properties of electron beam-rapid manufactured Ti–6Al–4V biomedical prototypes compared to wrought Ti–6Al–4V. *Mater. Charact.* **2009**, *60*, 96–105. [CrossRef]

30. Dinda, G.; Song, L.; Mazumder, J. Fabrication of Ti-6Al-4V scaffolds by direct metal deposition. *Metall. Mater. Trans. A* **2008**, *39*, 2914–2922. [CrossRef]

31. Tomus, D.; Qian, M.; Brice, C.A.; Muddle, B.C. Electron beam processing of Al–2Sc alloy for enhanced precipitation hardening. *Scr. Mater.* **2010**, *63*, 151–154. [CrossRef]

32. Haftlang, F.; Kim, H.S. A perspective on precipitation-hardening high-entropy alloys fabricated by additive manufacturing. *Mater. Des.* **2021**, *211*, 110161. [CrossRef]

33. Benoit, M.; Tabaie, S.; Waqar, T.; Ganton, T.; Amirkhiz, B.; Hadadzadeh, A.; Nasiri, A. Effects of additive manufacturing processes and isothermal aging on the microstructure and properties of 13-8 Mo precipitation hardening martensitic stainless steel. *Addit. Manuf.* **2023**, *72*, 103615. [CrossRef]

34. Zhang, W.; Chabok, A.; Wang, H.; Shen, J.; Oliveira, J.; Feng, S.; Schell, N.; Kooi, B.J.; Pei, Y. Ultra-strong and ductile precipitation-strengthened high entropy alloy with 0.5% Nb addition produced by laser additive manufacturing. *J. Mater. Sci. Technol.* **2024**, *187*, 195–211. [CrossRef]

35. Malinov, S.; Sha, W.; Guo, Z. Application of artificial neural network for prediction of time–temperature–transformation diagrams in titanium alloys. *Mater. Sci. Eng. A* **2000**, *283*, 1–10. [CrossRef]

36. Sun, Z.; Yang, H.; Tang, Z. Microstructural evolution model of TA15 titanium alloy based on BP neural network method and application in isothermal deformation. *Comput. Mater. Sci.* **2010**, *50*, 308–318. [CrossRef]

37. Sun, Z.; Wang, X.; Zhang, J.; Yang, H. Prediction and control of equiaxed α in near-β forging of TA15 Ti-alloy based on BP neural network: For purpose of tri-modal microstructure. *Mater. Sci. Eng. A* **2014**, *591*, 18–25. [CrossRef]

38. Malinov, S.; Sha, W.; McKeown, J. Modelling the correlation between processing parameters and properties in titanium alloys using artificial neural network. *Comput. Mater. Sci.* **2001**, *21*, 375–394. [CrossRef]

39. Malinov, S.; Sha, W.; Markovsky, P. Experimental study and computer modelling of the $\beta \Rightarrow \alpha+\beta$ phase transformation in β21s alloy at isothermal conditions. *J. Alloys Compd.* **2003**, *348*, 110–118. [CrossRef]

40. Fotovati, A.; Goswami, T. Prediction of elevated temperature fatigue crack growth rates in TI-6AL-4V alloy–neural network approach. *Mater. Des.* **2004**, *25*, 547–554. [CrossRef]

41. Collins, P.C.; Koduri, S.; Welk, B.; Tiley, J.; Fraser, H.L. Neural Networks Relating Alloy Composition, Microstructure, and Tensile Properties of α/β-Processed TIMETAL 6-4. *Metall. Mater. Trans. A* **2013**, *44*, 1441–1453. [CrossRef]

42. Yoo, Y.; Jo, C.; Jones, C. Compositional prediction of creep rupture life of single crystal Ni base superalloy by Bayesian neural network. *Mater. Sci. Eng. A* **2002**, *336*, 22–29. [CrossRef]

43. Bhadeshia, H. Design of ferritic creep-resistant steels. *ISIJ Int.* **2001**, *41*, 626–640. [CrossRef]

44. Genel, K. Application of artificial neural network for predicting strain-life fatigue properties of steels on the basis of tensile tests. *Int. J. Fatigue* **2004**, *26*, 1027–1035. [CrossRef]

45. Artymiak, P.; Bukowski, L.; Feliks, J.; Narberhaus, S.; Zenner, H. Determination of S–N curves with the application of artificial neural networks. *Fatigue Fract. Eng. Mater. Struct.* **1999**, *22*, 723–728.

46. Yescas, M. Prediction of the Vickers hardness in austempered ductile irons using neural networks. *Int. J. Cast Met. Res.* **2003**, *15*, 513–521. [CrossRef]

47. Cool, T.; Bhadeshia, H.; MacKay, D. The yield and ultimate tensile strength of steel welds. *Mater. Sci. Eng. A* **1997**, *223*, 186–200. [CrossRef]

48. Bhadeshia, H.; MacKay, D.; Svensson, L.-E. Impact toughness of C–Mn steel arc welds–Bayesian neural network analysis. *Mater. Sci. Technol.* **1995**, *11*, 1046–1051. [CrossRef]

49. Kasat, R.B.; Ray, A.K.; Gupta, S.K. Applications of genetic algorithm in polymer science and engineering. *Mater. Manuf. Process.* **2003**, *18*, 523–532. [CrossRef]

50. Santos, C.; Spim, J.; Garcia, A. Mathematical modeling and optimization strategies (genetic algorithm and knowledge base) applied to the continuous casting of steel. *Eng. Appl. Artif. Intell.* **2003**, *16*, 511–527. [CrossRef]

51. Kulkarni, A.J.; Krishnamurthy, K.; Deshmukh, S.; Mishra, R. Microstructural optimization of alloys using a genetic algorithm. *Mater. Sci. Eng. A* **2004**, *372*, 213–220. [CrossRef]

52. Chua, A.L.-S.; Benedek, N.A.; Chen, L.; Finnis, M.W.; Sutton, A.P. A genetic algorithm for predicting the structures of interfaces in multicomponent systems. *Nat. Mater.* **2010**, *9*, 418–422. [CrossRef] [PubMed]

53. Fu, Z.; Mo, J.; Chen, L.; Chen, W. Using genetic algorithm-back propagation neural network prediction and finite-element model simulation to optimize the process of multiple-step incremental air-bending forming of sheet metal. *Mater. Des.* **2010**, *31*, 267–277. [CrossRef]

54. Anijdan, S.; Bahrami, A.; Hosseini, H.; Shafyei, A. Using genetic algorithm and artificial neural network analyses to design an Al–Si casting alloy of minimum porosity. *Mater. Des.* **2006**, *27*, 605–609. [CrossRef]

55. Somashekhar, K.; Ramachandran, N.; Mathew, J. Optimization of material removal rate in micro-EDM using artificial neural network and genetic algorithms. *Mater. Manuf. Process.* **2010**, *25*, 467–475. [CrossRef]

56. Song, R.; Zhang, Q. Heat treatment optimization for 7175 aluminum alloy by genetic algorithm. *Mater. Sci. Eng. C* **2001**, *17*, 133–137. [CrossRef]

57. Collins, P.; Koduri, S.; Dixit, V.; Fraser, H. Understanding the interdependencies between composition, microstructure, and continuum variables and their influence on the fracture toughness of α/β-processed Ti-6Al-4V. *Metall. Mater. Trans. A* **2018**, *49*, 848–863. [CrossRef]

58. Kusano, M.; Miyazaki, S.; Watanabe, M.; Kishimoto, S.; Bulgarevich, D.S.; Ono, Y.; Yumoto, A. Tensile properties prediction by multiple linear regression analysis for selective laser melted and post heat-treated Ti-6Al-4V with microstructural quantification. *Mater. Sci. Eng. A* **2020**, *787*, 139549. [CrossRef]

59. Soar, P.; Palanca, M.; Dall'Ara, E.; Tozzi, G. Data-driven image mechanics (D2IM): A deep learning approach to predict displacement and strain fields from undeformed X-ray tomography images–Evaluation of bone mechanics. *Extrem. Mech. Lett.* **2024**, *71*, 102202. [CrossRef]

60. Kopp, R.; Joseph, J.; Ni, X.; Roy, N.; Wardle, B.L. Deep Learning Unlocks X-ray Microtomography Segmentation of Multiclass Microdamage in Heterogeneous Materials. *Adv. Mater.* **2022**, *34*, 2107817. [CrossRef] [PubMed]

61. Ren, Z.; Gao, L.; Clark, S.J.; Fezzaa, K.; Shevchenko, P.; Choi, A.; Everhart, W.; Rollett, A.D.; Chen, L.; Sun, T. Machine learning–aided real-time detection of keyhole pore generation in laser powder bed fusion. *Science* **2023**, *379*, 89–94. [CrossRef] [PubMed]

62. Rezasefat, M.; Li, H.; Hogan, J.D. Prediction of microstructural-dependent mechanical properties, progressive damage, and stress distribution from X-ray computed tomography scans using a deep learning workflow. *Comput. Methods Appl. Mech. Eng.* **2024**, *424*, 116878. [CrossRef]

63. Herriott, C.; Spear, A.D. Predicting microstructure-dependent mechanical properties in additively manufactured metals with machine-and deep-learning methods. *Comput. Mater. Sci.* **2020**, *175*, 109599. [CrossRef]

64. Ye, S.; Li, B.; Li, Q.; Zhao, H.-P.; Feng, X.-Q. Deep neural network method for predicting the mechanical properties of composites. *Appl. Phys. Lett.* **2019**, *115*, 161901. [CrossRef]

65. Dai, W.; Wang, H.; Guan, Q.; Li, D.; Peng, Y.; Tomé, C.N. Studying the micromechanical behaviors of a polycrystalline metal by artificial neural networks. *Acta Mater.* **2021**, *214*, 117006. [CrossRef]

66. Mackay, D.J. Bayesian Methods for Adaptive Methods. Ph.D. Thesis, California Institute of Technology, Pasadena, CA, USA, 1992.

67. MacKay, D.J. A practical Bayesian framework for backpropagation networks. *Neural Comput.* **1992**, *4*, 448–472. [CrossRef]

68. Mentges, N.; Dashtbozorg, B.; Mirkhalaf, S. A micromechanics-based artificial neural networks model for elastic properties of short fiber composites. *Compos. Part B Eng.* **2021**, *213*, 108736. [CrossRef]

69. Goh, C.H.; Dachowicz, A.P.; Collins, P.C.; Allen, J.K.; Mistree, F. Predicting Constitutive Equations for Materials Design: A Conceptual Exposition. In *Integrated Computational Materials Engineering (ICME) for Metals*; John Wiley & Sons, Inc.: Hoboken, NJ, USA, 2018; pp. 515–538.

70. Hayes, B.J.; Martin, B.W.; Welk, B.; Kuhr, S.; Ales, T.K.; Brice, D.A.; Ghamarian, I.; Baker, A.H.; Haden, C.V.; Harlow, G.; et al. Predicting tensile properties of Ti-6Al-4V produced via directed energy deposition. *Acta Mater.* **2017**, *133*, 120–133. [CrossRef]

71. Xie, X.; Samaei, A.; Guo, J.; Liu, W.K.; Gan, Z. Data-driven discovery of dimensionless numbers and governing laws from scarce measurements. *Nat. Commun.* **2022**, *13*, 7562. [CrossRef] [PubMed]

72. Pilania, G. Machine learning in materials science: From explainable predictions to autonomous design. *Comput. Mater. Sci.* **2021**, *193*, 110360. [CrossRef]

73. Ghamarian, I.; Samimi, P.; Dixit, V.; Collins, P.C. A constitutive equation relating composition and microstructure to properties in Ti-6Al-4V: As derived using a novel integrated computational approach. *Metall. Mater. Trans. A* **2015**, *46*, 5021–5037. [CrossRef]

74. Ghamarian, I.; Hayes, B.; Samini, P.; Welk, B.; Fraser, H.; Collins, P. Developing a phenomenological equation to predict yield strength from composition and microstructure in β processed Ti-6Al-4V. *Mater. Sci. Eng. A* **2016**, *660*, 172–180. [CrossRef]